

# A Valence Bond Perspective on the Molecular Shapes of Simple Metal Alkyls and Hydrides

Clark R. Landis,\* Timothy K. Firman, Daniel M. Root, and Thomas Cleveland

Contribution from the Department of Chemistry, University of Wisconsin—Madison, 1101 University Avenue, Madison, Wisconsin 53706

Received March 31, 1997. Revised Manuscript Received August 18, 1997

**Abstract:** Many chemists use qualitative valence bond concepts to rationalize molecular structures and properties, particularly for main group elements. Extension of Pauling's valence bond concepts to transition metal compounds dominated by covalent bonding leads to simple prescriptions for determining bond hybridizations and molecular shapes. As a result, transition metal structures can be discussed in the familiar terminology of Lewis structures, lone pairs, hybrid orbitals, hypervalence, and resonance. A primary feature of these prescriptions is the relative impotence of valence p-orbitals in the formation of covalent bonds at transition metals:  $sd^n$  hybridization dominates. This feature is consistent with detailed analyses of high level quantum mechanical computations. Unlike Pauling's original treatments of hypervalency, rationalization of empirical structures and high level electronic structure computational results requires consideration of multiple resonance structures. Valence bond theory constitutes a compact and powerful model that accurately explains the often unexpected structures observed for simple metal alkyls and hydrides.

## I. Introduction

The rationalization of experimentally observed molecular shapes has provided a driving force for the development of theoretical models of chemical bonding since the original conception of valence bond (VB) theory by Heitler, London, Pauling, and Slater in the late 1920s.<sup>1</sup> For example, the construct of  $sp^3$  hybridization arose largely from the desire to unite emerging quantum concepts with the known tetrahedral structure of methane. Recently we have shown that molecular mechanics algorithms (VALBOND) for normal valent molecules of the p-block,<sup>2</sup> hypervalent molecules of the p-block,<sup>3</sup> and some simple transition metal hydrides and alkyls<sup>4</sup> are readily derived from VB theory.

Qualitative VB theory invokes hybridization and resonance as the primary bases for rationalizing molecular shapes. A rich body of literature describes the correlation of hybridization with molecular structures and properties, particularly for the main group elements.<sup>5–8</sup> A drawback of hybrid orbitals is that they do not correspond to stationary quantum states and, hence, do not form a convenient basis for understanding observed properties such as photoelectron spectra. Nonetheless, schemes for the localization of electron density such as Weinhold's NBO

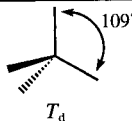
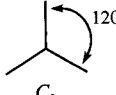
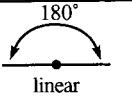
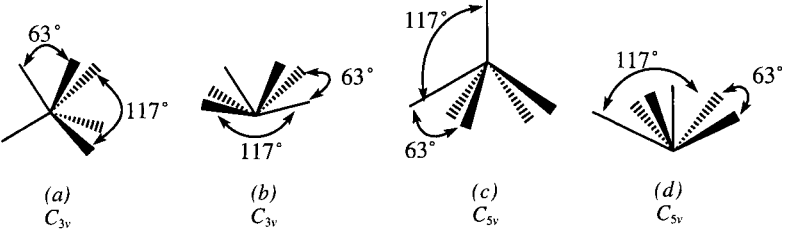
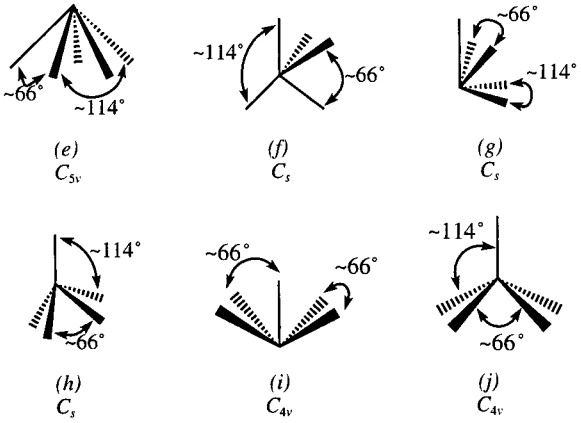
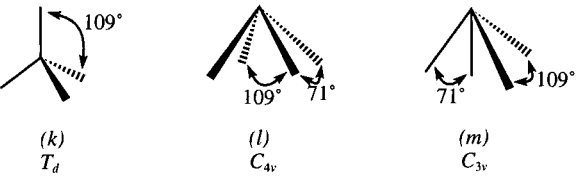
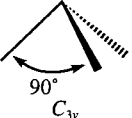
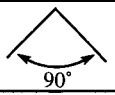
method<sup>6,7,9–13</sup> demonstrate that hybridized local bonds are good descriptors of electron density distributions derived from electronic structure calculations for many molecules.

For nonhypervalent molecules of the p-block, common  $sp^1$ ,  $sp^2$ , and  $sp^3$  hybridizations are determined directly from Lewis structures. Fine adjustments in hybridization with use of Bent's rule<sup>5</sup> provide a mechanism for rationalizing structural deviations from idealized  $sp$ -,  $sp^2$ -, and  $sp^3$ -derived geometries. Historically, the geometries of transition metal complexes and hypervalent main group compounds have been rationalized through the use of  $sp^m d^n$  hybridization.<sup>14,15</sup> However, analyses of electron density distributions from high level ab initio computations, such as Magnusson's definitive study on hypervalency,<sup>16</sup> do not support the participation of d orbitals in the hybridization of main group elements. Analogously, we and others<sup>17–22</sup> have

(1) Pauling, L. *Proc. Natl. Acad. Sci. U.S.A.* **1928**, *14*, 359–362.  
 (2) Root, D. M.; Landis, C. R.; Cleveland, T. *J. Am. Chem. Soc.* **1993**, *115*, 4201–4209.  
 (3) Cleveland, T.; Landis, C. R. *J. Am. Chem. Soc.* **1996**, *118*, 6020–6030.  
 (4) Landis, C. R.; Cleveland, T.; Firman, T. K. *J. Am. Chem. Soc.* **1995**, *117*, 1859–1860.  
 (5) Bent, H. *Chem. Rev. (Washington, D.C.)* **1961**, *61*, 275–311.  
 (6) Carpenter, J. E.; Weinhold, F. *J. Am. Chem. Soc.* **1988**, *110*, 368–372.  
 (7) Foster, J. P.; Weinhold, F. *J. Am. Chem. Soc.* **1980**, *102*, 7211–7218.  
 (8) Maksic, Z. B., Ed. *Directional Properties of Covalent Bonds in Molecules*; Springer-Verlag: Berlin, 1990; Vol. 2.

(9) Reed, A. E.; Weinstock, R. B.; Weinhold, F. *J. Chem. Phys.* **1985**, *83*, 735–746.  
 (10) Reed, A. E.; Weinhold, F. *J. Chem. Phys.* **1985**, *83*, 1736–1740.  
 (11) Reed, A. E.; Weinhold, F.; Curtiss, L. A.; Pochatko, D. J. *J. Chem. Phys.* **1986**, *84*, 5687–5705.  
 (12) Glendening, E. D.; Badenhop, J. K.; Reed, A. E.; Carpenter, J. E.; Weinhold, F.; University of Wisconsin: Madison, WI, 1994.  
 (13) Glendening, E. D.; Weinhold, F. *Natural Resonance Theory. I. General Formalism*; University of Wisconsin Theoretical Chemistry Institute, 1994.  
 (14) Pauling, L. *The Nature of the Chemical Bond*; Cornell University: Ithaca, 1960.  
 (15) Pauling, L. *Proc. Natl. Acad. Sci. U.S.A.* **1975**, *72*, 4200–4202.  
 (16) Magnusson, E. *J. Am. Chem. Soc.* **1990**, *112*, 7940–7951.  
 (17) Langhoff, S. R.; Bauschlicher, C. W. *Annu. Rev. Phys. Chem.* **1988**, *39*, 181–212.  
 (18) Ohanessian, G.; Goddard, W. A. *Acc. Chem. Res.* **1990**, *23*, 386–392.  
 (19) Ohanessian, G.; Brusich, M. J.; Goddard, W. A. *J. Am. Chem. Soc.* **1990**, *112*, 7179–7189.  
 (20) Shen, M.; Schaefer, H. F.; Partridge, H. *J. Chem. Phys.* **1992**, *98*, 508–521.  
 (21) Ma, B. Y.; Collins, C. L.; Schaefer, H. F. *J. Am. Chem. Soc.* **1996**, *118*, 870–879.  
 (22) Dobbs, K. D.; Hehre, W. J. *J. Am. Chem. Soc.* **1986**, *108*, 4663–4664.

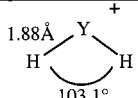
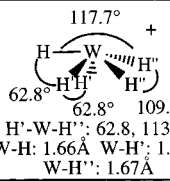
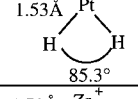
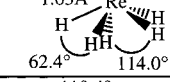
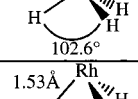
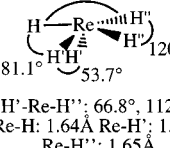
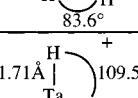
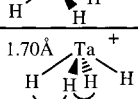
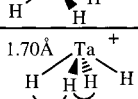
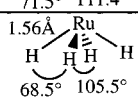
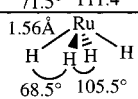
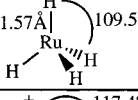
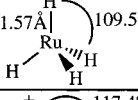
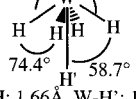
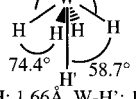
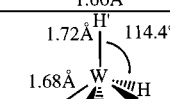
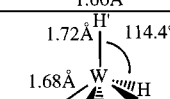
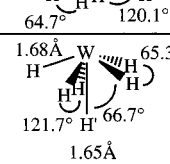
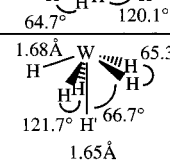


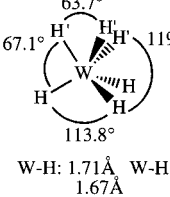
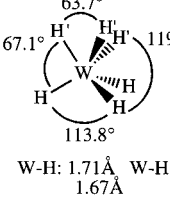
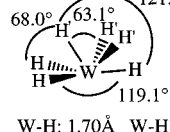
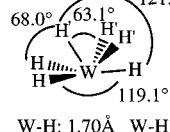
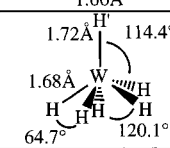
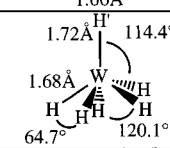
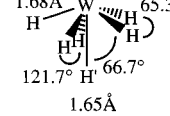
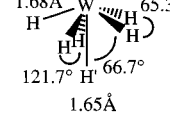
**Table 1.** Molecular Shapes Associated with Different Bond Hybridizations

Idealized Hybridization and Angles	Idealized Molecular Shape	Examples of Indicated Formal Hybridization
sp <sup>3</sup> 109.5°	 <i>T<sub>d</sub></i>	CH <sub>4</sub>
sp <sup>2</sup> 120°	 <i>C<sub>3v</sub></i>	BCl <sub>3</sub>
sp 180°	 linear	C <sub>2</sub> H <sub>2</sub>
sd <sup>5</sup> 117° and 63°	 (a) <i>C<sub>3v</sub></i> (b) <i>C<sub>3v</sub></i> (c) <i>C<sub>5v</sub></i> (d) <i>C<sub>5v</sub></i>	Computational: WH <sub>6</sub> , <sup>20,26</sup> [TcH <sub>6</sub> ] <sup>+</sup> 4 Experimental: W(Me) <sub>6</sub> , <sup>52,53</sup> [Zr(Me) <sub>6</sub> ] <sup>2-</sup> , <sup>54</sup> W(o-Xylidene) <sub>3</sub> <sup>55</sup>
sd <sup>4</sup> 114° and 66°	 (e) <i>C<sub>5v</sub></i> (f) <i>C<sub>s</sub></i> (g) <i>C<sub>s</sub></i> (h) <i>C<sub>s</sub></i> (i) <i>C<sub>4v</sub></i> (j) <i>C<sub>4v</sub></i>	Computational: [WH <sub>5</sub> ] <sup>+</sup> , ReH <sub>5</sub> Experimental: Ta(Me) <sub>5</sub> , <sup>56</sup> Ta(CH <sub>2</sub> -p-Tol) <sub>5</sub> <sup>57</sup>
sd <sup>3</sup> 109° and 71°	 (k) <i>T<sub>d</sub></i> (l) <i>C<sub>4v</sub></i> (m) <i>C<sub>3v</sub></i>	Computational: RuH <sub>4</sub> , [TaH <sub>4</sub> ] <sup>+</sup> Experimental: Os(Ph) <sub>4</sub> , <sup>58</sup> Mo(Nor) <sub>4</sub> , <sup>60</sup> Cr(2,2-dimethyl,1-phenylethenyl) <sub>4</sub> , <sup>61</sup> [Os(o-Tol) <sub>4</sub> ] <sup>+</sup> , <sup>62</sup> Os(o-Tol) <sub>4</sub> , <sup>64</sup> Re(o-Tol) <sub>4</sub> , <sup>63</sup> Ru(o-Tol) <sub>4</sub> , <sup>63</sup> Mo(o-Tol) <sub>4</sub> , <sup>59</sup> Ru(C <sub>6</sub> H <sub>11</sub> ) <sub>4</sub> , <sup>58</sup> Os(C <sub>6</sub> H <sub>11</sub> ) <sub>4</sub> , <sup>58</sup> Cr(C <sub>6</sub> H <sub>11</sub> ) <sub>4</sub> , <sup>58</sup> Ru(Mes) <sub>4</sub> , <sup>65</sup> [Ir(Mes) <sub>4</sub> ] <sup>+</sup> 65
sd <sup>2</sup> 90°	 <i>C<sub>3v</sub></i>	Computational: RhH <sub>3</sub> <sup>12</sup> , [ZrH <sub>3</sub> ] <sup>+</sup> 12 Experimental: La(CH(SiMe <sub>3</sub> ) <sub>2</sub> ) <sub>3</sub> , <sup>66</sup> Rh(Mes) <sub>3</sub> , <sup>67</sup> Ir(Mes) <sub>3</sub> <sup>65</sup>
sd 90°	 90°	Computational: Pt(Me) <sub>2</sub> , PtH <sub>2</sub>

presented evidence that p-orbitals do not significantly participate in the formation of covalent bonds at transition metals.<sup>4</sup>

In this paper we describe the general methods of a revised qualitative VB theory of molecular shapes. This work has been

Table 2. DFT(B3LYP) and NBO Results for Normal and Hypovalent Metal Hydrides

Compound (Relative Energy)	Optimized Geometry	Non-Lewis Density	Natural Charges	NBO Bond Hybridizations and (Polarities)	Compound (Relative Energy)	Optimized Geometry	Non-Lewis Density	Natural Charges	NBO Bond Hybridizations and (Polarities)
[YH <sub>2</sub> ] <sup>+</sup> (C <sub>2v</sub> )		0.03%	Y: +1.91 H: -0.45	Y-H: sd <sup>2.27</sup> p <sup>0.03</sup> (27% Y: 73% H)	[WH <sub>3</sub> ] <sup>+</sup> (C <sub>3v</sub> , g)		0.4%	W: +0.82 H: +0.01 H': -0.01 H'': +0.09	W-H: sd <sup>5.06</sup> p <sup>0.02</sup> (51% W: 49% H') W-H': sd <sup>3.87</sup> p <sup>0.01</sup> (50% W: 50% H) W-H'': sd <sup>4.33</sup> p <sup>0.01</sup> (55% W: 45% H) Avg.: sd <sup>4.26</sup> p <sup>0.01</sup>
PtH <sub>2</sub> (C <sub>2v</sub> )		0.10%	Pt: -0.16 H: +0.08	Pt-H: sd <sup>1.25</sup> p <sup>0.00</sup> (55% Pt: 45% H)	ReH <sub>5</sub> (C <sub>5v</sub> , e)		0.6%	Re: -0.12 H: +0.02	Re-H: sd <sup>4.18</sup> p <sup>0.01</sup> (52% Re: 48% H)
[ZrH <sub>3</sub> ] <sup>+</sup> (C <sub>3v</sub> )		0.13%	Zr: +1.74 H: -0.25	Zr-H: sd <sup>2.45</sup> p <sup>0.01</sup> (38% Zr: 62% H)	ReH <sub>5</sub> (C <sub>v</sub> , g)		0.4%	Re: -0.01 H: -0.04 H'': +0.08	Re-H: sd <sup>3.34</sup> p <sup>0.02</sup> (48% Re: 52% H) Re-H': sd <sup>4.26</sup> p <sup>0.02</sup> (48% Re: 52% H') Re-H'': sd <sup>4.14</sup> p <sup>0.01</sup> (54% Re: 46% H'') Avg.: sd <sup>4.02</sup> p <sup>0.02</sup>
RhH <sub>3</sub> (C <sub>3v</sub> )		0.5%	Rh: -0.18 H: +0.06	Rh-H: sd <sup>2.00</sup> p <sup>0.01</sup> (54% Rh: 46% H)	[TaH <sub>4</sub> ] <sup>+</sup> (T <sub>d</sub> )		0.06%	Ta: +1.60 H: -0.15	Ta-H: sd <sup>2.99</sup> p <sup>0.01</sup> (43% Ta: 57% H)
[TaH <sub>4</sub> ] <sup>+</sup> (T <sub>d</sub> )		0.06%	Ta: +1.60 H: -0.15	Ta-H: sd <sup>2.99</sup> p <sup>0.01</sup> (43% Ta: 57% H)	[TaH <sub>4</sub> ] <sup>+</sup> (C <sub>4v</sub> )		0.18%	Ta: +1.36 H: -0.09	Ta-H: sd <sup>2.99</sup> p <sup>0.01</sup> (46% Ta: 54% H)
[TaH <sub>4</sub> ] <sup>+</sup> (C <sub>4v</sub> )		0.18%	Ta: +1.36 H: -0.09	Ta-H: sd <sup>2.99</sup> p <sup>0.01</sup> (46% Ta: 54% H)	RuH <sub>4</sub> (C <sub>4v</sub> )		0.8%	Ru: -0.33 H: +0.08	Ru-H: sd <sup>2.99</sup> p <sup>0.01</sup> (55% Ru: 45% H)
RuH <sub>4</sub> (C <sub>4v</sub> )		0.8%	Ru: -0.33 H: +0.08	Ru-H: sd <sup>2.99</sup> p <sup>0.01</sup> (55% Ru: 45% H)	RuH <sub>4</sub> (T <sub>d</sub> )		0.2%	Ru: -0.18 H: +0.05	Ru-H: sd <sup>3.00</sup> p <sup>0.00</sup> (53% Ru: 47% H)
RuH <sub>4</sub> (T <sub>d</sub> )		0.2%	Ru: -0.18 H: +0.05	Ru-H: sd <sup>3.00</sup> p <sup>0.00</sup> (53% Ru: 47% H)	[WH <sub>3</sub> ] <sup>+</sup> (C <sub>4v</sub> , i)		0.5%	W: +0.72 H: +0.03 H': +0.15	W-H: sd <sup>3.80</sup> p <sup>0.01</sup> (52% W: 48% H') W-H': sd <sup>4.94</sup> p <sup>0.01</sup> (58% W: 42% H) Avg.: sd <sup>3.99</sup> p <sup>0.01</sup>
[WH <sub>3</sub> ] <sup>+</sup> (C <sub>4v</sub> , i)		0.5%	W: +0.72 H: +0.03 H': +0.15	W-H: sd <sup>3.80</sup> p <sup>0.01</sup> (52% W: 48% H') W-H': sd <sup>4.94</sup> p <sup>0.01</sup> (58% W: 42% H) Avg.: sd <sup>3.99</sup> p <sup>0.01</sup>	[WH <sub>5</sub> ] <sup>+</sup> (C <sub>v</sub> , h)		0.3%	W: +0.96 H: -0.04 H': +0.05 H'': 0.00	W-H: sd <sup>4.08</sup> p <sup>0.01</sup> (48% W: 52% H') W-H': sd <sup>4.37</sup> p <sup>0.01</sup> (53% W: 47% H) W-H'': sd <sup>4.24</sup> p <sup>0.01</sup> (50% W: 50% H) Avg.: sd <sup>4.26</sup> p <sup>0.01</sup>
[WH <sub>5</sub> ] <sup>+</sup> (C <sub>v</sub> , h)		0.3%	W: +0.96 H: -0.04 H': +0.05 H'': 0.00	W-H: sd <sup>4.08</sup> p <sup>0.01</sup> (48% W: 52% H') W-H': sd <sup>4.37</sup> p <sup>0.01</sup> (53% W: 47% H) W-H'': sd <sup>4.24</sup> p <sup>0.01</sup> (50% W: 50% H) Avg.: sd <sup>4.26</sup> p <sup>0.01</sup>	[WH <sub>5</sub> ] <sup>+</sup> (C <sub>4v</sub> , j)		0.2%	W: +0.99 H: +0.01 H': -0.03	W-H: sd <sup>3.80</sup> p <sup>0.01</sup> (51% W: 49% H') W-H': sd <sup>5.20</sup> p <sup>0.01</sup> (49% W: 51% H) Avg.: sd <sup>3.99</sup> p <sup>0.01</sup>
[WH <sub>5</sub> ] <sup>+</sup> (C <sub>4v</sub> , j)		0.2%	W: +0.99 H: +0.01 H': -0.03	W-H: sd <sup>3.80</sup> p <sup>0.01</sup> (51% W: 49% H') W-H': sd <sup>5.20</sup> p <sup>0.01</sup> (49% W: 51% H) Avg.: sd <sup>3.99</sup> p <sup>0.01</sup>	WH <sub>6</sub> (C <sub>3v</sub> , a)		0.5%	W: +0.40 H: -0.13 H': +0.00	W-H: sd <sup>4.08</sup> p <sup>0.01</sup> (43% W: 57% H) W-H': sd <sup>6.27</sup> p <sup>0.02</sup> (50% W: 50% H') Avg.: sd <sup>4.88</sup> p <sup>0.02</sup>
WH <sub>6</sub> (C <sub>3v</sub> , a)		0.5%	W: +0.40 H: -0.13 H': +0.00	W-H: sd <sup>4.08</sup> p <sup>0.01</sup> (43% W: 57% H) W-H': sd <sup>6.27</sup> p <sup>0.02</sup> (50% W: 50% H') Avg.: sd <sup>4.88</sup> p <sup>0.02</sup>	WH <sub>6</sub> (C <sub>3v</sub> , b)		0.6%	W: +0.19 H: -0.12 H': +0.06	W-H: sd <sup>4.48</sup> p <sup>0.02</sup> (44% W: 56% H) W-H': sd <sup>5.58</sup> p <sup>0.01</sup> (53% W: 47% H') Avg.: sd <sup>4.98</sup> p <sup>0.02</sup>
WH <sub>6</sub> (C <sub>3v</sub> , b)		0.6%	W: +0.19 H: -0.12 H': +0.06	W-H: sd <sup>4.48</sup> p <sup>0.02</sup> (44% W: 56% H) W-H': sd <sup>5.58</sup> p <sup>0.01</sup> (53% W: 47% H') Avg.: sd <sup>4.98</sup> p <sup>0.02</sup>	WH <sub>6</sub> (C <sub>3v</sub> , c)		0.4%	W: +0.41 H: -0.05 H': -0.17	W-H: sd <sup>5.43</sup> p <sup>0.01</sup> (48% W: 52% H) W-H': sd <sup>3.45</sup> p <sup>0.01</sup> (41% W: 59% H') Avg.: sd <sup>4.99</sup> p <sup>0.01</sup>
WH <sub>6</sub> (C <sub>3v</sub> , c)		0.4%	W: +0.41 H: -0.05 H': -0.17	W-H: sd <sup>5.43</sup> p <sup>0.01</sup> (48% W: 52% H) W-H': sd <sup>3.45</sup> p <sup>0.01</sup> (41% W: 59% H') Avg.: sd <sup>4.99</sup> p <sup>0.01</sup>	WH <sub>6</sub> (C <sub>3v</sub> , d)		0.6%	W: +0.01 H: -0.03 H': +0.15	W-H: sd <sup>5.10</sup> p <sup>0.02</sup> (49% W: 51% H) W-H': sd <sup>4.45</sup> p <sup>0.00</sup> (58% W: 42% H') Avg.: sd <sup>4.98</sup> p <sup>0.02</sup>
WH <sub>6</sub> (C <sub>3v</sub> , d)		0.6%	W: +0.01 H: -0.03 H': +0.15	W-H: sd <sup>5.10</sup> p <sup>0.02</sup> (49% W: 51% H) W-H': sd <sup>4.45</sup> p <sup>0.00</sup> (58% W: 42% H') Avg.: sd <sup>4.98</sup> p <sup>0.02</sup>					

stimulated by the recent observation of transition metal alkyls (e.g.,  $W(CH_3)_6$ <sup>23–25</sup>) and hydrides (e.g.,  $WH_6$ <sup>20,26,27</sup>) which computation and experiment show to adopt complex, non-VSEPR<sup>28</sup> structures. We show that the concepts of hybridization and resonance form the basis of a general method for understanding the shapes of molecules throughout the periodic table. This method (1) is consistent with electron density distributions obtained from high level ab initio computations, (2) rationalizes many fine details of molecular shapes, and (3) leads to unique insights into the origin of the irregular shapes of metal hydrides and alkyls. This work represents an extension and generalization of the VB concepts first proposed by Pauling 66 years ago.<sup>29</sup>

The plan of this paper is to first define and discuss the rules for estimating bond hybridizations and the orbital shapes associated with simple covalent molecules. Next we address the additional considerations used in applying VB concepts to hypervalent molecules. Finally, we explore the influence of core polarizations on transition metal structures, the limitations of simple VB concepts, extensions of VB principles to more ionic bonding situations, a generalization of Bent's rule based on ionic-covalent resonance, and a VB-based interpretation of the trans influence.

## II. Computational Methods

Many of the metal hydrides discussed in this paper have not been structurally characterized or even synthesized. However, we note that there is a growing body of experimental evidence for the existence and geometries of simple metal hydrides resulting from matrix isolation studies.<sup>30–33</sup> We have modeled the geometries with Gaussian 94,<sup>34</sup> using Density Functional Theory (DFT). Becke's 3-parameter functional (B3)<sup>35</sup> was used, with Lee, Yang, and Parr<sup>36</sup> (LYP) correlation energies. This method, DFT(B3LYP), has been shown to have accuracy comparable to sophisticated post-Hartree-Fock methods for transition metals<sup>37</sup> and their monohydrides.<sup>38</sup> The double- $\zeta$  LANL2DZ basis sets and effective core potentials (for all but valence and the first subvalence shells) developed by Hay and Wadt<sup>39–42</sup> were used except where otherwise noted in the text. All reported geometries are true minima as determined by the absence of any negative eigenvalues in the vibrational frequency analysis.

There is always some concern as to whether the basis sets and computational levels employed are sufficiently accurate to support the

(23) Landis, C. R.; Cleveland, T.; Firman, T. K. *Science* **1996**, *272*, 179.

(24) Pfennig, V.; Seppelt, K. *Science* **1996**, *271*, 626–628.

(25) Kaupp, M. *J. Am. Chem. Soc.* **1996**, *118*, 3018–3024.

(26) Kang, S. K.; Tang, H.; Albright, T. A. *J. Am. Chem. Soc.* **1993**, *115*, 1971–1981.

(27) Tanpipat, N.; Baker, J. J. *Phys. Chem.* **1996**, *100*, 19818–19823.

(28) Gillespie, R. J.; Hargittai, I. *The VSEPR Model of Molecular Geometry*; Allyn and Bacon: Boston, 1991.

(29) Pauling, L. *J. Am. Chem. Soc.* **1931**, *53*, 1367–1400.

(30) Chertihin, G. V.; Andrews, L. *J. Am. Chem. Soc.* **1995**, *117*, 6402–6403.

(31) Billups, W. E.; Chang, S. C.; Hauge, R. H.; Margrave, J. L. *J. Am. Chem. Soc.* **1995**, *117*, 1387–1392.

(32) Chertihin, G. V.; Andrews, L. *J. Phys. Chem.* **1995**, *99*, 12131–12134.

(33) Chertihin, G. V.; Andrews, L. *J. Phys. Chem.* **1995**, *99*, 15004–15010.

(34) Frisch, M. J.; Trucks, G. W.; Schlegel, H. B.; Gill, P. M. W.; Johnson, B. G.; Robb, M. A.; Cheeseman, J. R.; Keith, T.; Petersson, G. A.; Montgomery, J. A.; Raghavachari, K.; Al-Laham, M. A.; Zakrzewski, V. G.; Ortiz, J. V.; Foresman, J. B.; Cioslowski, J.; Stefanov, B. B.; Nanayakkara, A.; Challacombe, M.; Peng, C. Y.; Ayala, P. Y.; Chen, W.; Wong, M. W.; Andres, J. L.; Replogle, E. S.; Gomperts, R.; Martin, R. L.; Fox, D. J.; Binkley, J. S.; Defrees, D. J.; Baker, J.; Stewart, J. P.; Head-Gordon, M.; Gonzalez, C.; Pople, J. A.; Gaussian, Inc.: Pittsburgh, PA, 1995.

(35) Becke, A. D. *Phys. Rev. A* **1988**, *38*, 3098.

(36) Lee, C.; Yang, W.; Parr, R. G. *Phys. Rev. B* **1988**, *37*, 785–789.

(37) Jursic, B. S. *Int. J. Quantum Chem.* **1997**, *61*, 93–100.

(38) Barone, V.; Adamo, C. *Int. J. Quantum Chem.* **1997**, *61*, 443–451.

(39) Hay, P. J.; Wadt, W. R. *J. Chem. Phys.* **1985**, *82*, 271–284.

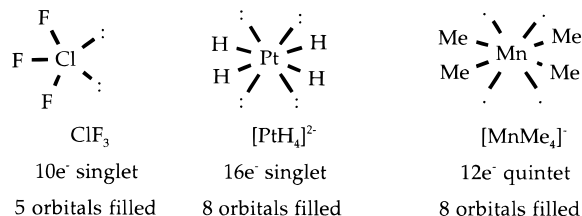
(40) Hay, P. J.; Wadt, W. R. *J. Chem. Phys.* **1985**, *82*, 285–298.

conclusions. For most of the metal hydrides reported here, we have performed computations at the HF, MP2, and GVB level. In general, the geometries of the resulting structures are essentially the same as those obtained for the DFT(B3LYP) computations. A detailed comparison of the energies of different isomers of  $WH_6$  obtained in our computations with those obtained by other high-level computations is given in Table 2. We conclude that the use of the DFT(B3LYP) method with effective core potential for all but the valence and first subvalence shells and double- $\zeta$  basis sets leads to energies that are essentially the same as other correlation-corrected computations such as QCISD(T).

## III. Rules for Approximating Bond Hybridizations

Although the procedures for determining the approximate hybridizations for nonhypervalent main group molecules are well established, the procedures for transition metals, and for hypervalent molecules of both the p- and d-block, are not. The terms hypovalent (electron deficient), hypervalent (electron surplus), and normal valent (or electron precise) are controversial.<sup>43–48</sup> For our discussion we use the terms as follows: For central atoms from the p-block, only the valence s and p orbitals are accessible. Molecules in which all four valence orbitals are doubly or singly occupied (e.g.,  $CH_4$  and triplet  $CH_2$ ) are normal valent. If not all valence orbitals are occupied, e.g., monomeric  $BH_3$  and singlet  $CH_2$ , then the molecule is termed hypovalent. Hypervalent molecules have Lewis structures that overfill the available valence orbitals, for example,  $XeF_2$  and  $ClF_3$ . We note that this use of the term hypervalency is consistent with that originally defined by Musher.<sup>49,50</sup> By these criteria, nonradical molecules with a p-block central atom are hypervalent if the electron count exceeds 8 electrons and hypovalent if the count is less than 8 electrons.

For the transition elements engaged in covalent bonding, only the valence s and the five d orbitals participate significantly in bonding. Normal valent molecules occupy each of these six valence orbitals; examples include  $WMe_6$ ,  $PtH_2$ , and triplet  $WH_4$ . Hypovalent examples from the d-block include  $Zr(CH_2Ph)_4$ ,  $Ta(CH_3)_5$ , and singlet  $W(Norbornyl)_4$ . Most common transition metal complexes are hypervalent: some examples of hypervalent metal hydrides and alkyls include  $[WMe_7]^{1-}$ ,  $[PtH_4]^{2-}$ ,  $[MnMe_4]^{1-}$ , and  $ReMe_6$ . By these criteria and Musher's definition, nonradical molecules with a d-block central atom are hypervalent if the electron count exceeds 12 electrons and hypovalent if the count is less than 12 electrons. Examples of hypervalent Lewis structures are shown below.



Viewed from a VB perspective, molecular geometry is controlled by the hybridizations of the bond forming orbitals. In general, bond forming orbitals at a central atom arrange so that overlap is minimized (e.g.,  $sp^3$  hybrids have zero overlap at  $109.5^\circ$ ). Hybridization of these orbitals is controlled by the total electron count and the nature of the ligands to which electron pair bonds are formed. Thus, the prediction of molecular shapes requires electron counting schemes that

prescribe appropriate hybridizations and resonance configurations. The following rules summarize such a prescription:

**Rule 1.** The s-block and p-block elements form  $sp^n$  hybrids, whereas d-block elements form  $sd^n$  hybrids.

Here “ $n$ ” is defined as the number of occupied orbitals minus one. We will call such hybridizations the *gross hybridization* of the central atom. Gross central atom hybridizations of some normal valent and hypovalent molecules are as follows:  $CH_4$  ( $sp^3$ ), triplet  $CH_2$  ( $sp^3$ ),  $BH_3$  ( $sp^2$ ), singlet  $CH_2$  ( $sp^2$ ),  $WMe_6$  ( $sd^5$ ),  $PtH_2$  ( $sd^5$ ), triplet  $WH_4$  ( $sd^5$ ),  $ZrH_4$  ( $sd^3$ ),  $TaH_5$  ( $sd^4$ ), and singlet  $WH_4$  ( $sd^4$ ).

**Rule 2.** For molecules with mixed ligands, lone pairs, radicals, and/or multiple bonds, the distribution of p or d character among the hybrid orbitals depends on the relative electronegativities of the ligands (Bent’s rule<sup>5</sup>) and the bond orders.

More specifically, the following empirical corollaries yield good approximations to hybrid orbital preferences: (i) lone pairs of the p-block elements prefer s-character; lone pairs of the d-block elements have essentially pure d-character; (ii) singly occupied orbitals of the p-block elements have a greater preference for p-character than most ligand bonds, and radical orbitals of d-block elements have essentially pure d-character; (iii)  $\pi$ -bonds at p-block elements are pure p-character; and (iv) main group compounds follow Bent’s rule.

In reference to main group compounds, Bent’s rule states that “Atomic s character concentrates in orbitals directed toward electropositive substituents”.<sup>5</sup> For example, the geometry of  $BF_2H$  is consistent with approximately  $sp^{2.1}$  hybridization in the B–F bonds and  $sp^{1.8}$  hybridization in the B–H bond. (An  $sp^{2.1}$  hybrid has 2.1 times as much p-character as it does s-character, or 68% p-character.) Natural Bond Orbital (NBO) analyses of ab initio electron densities<sup>6</sup> consistently support the implications of Bent’s rule.

Lone pairs and radicals can be considered to be bonded to very electropositive ligands. In accordance with Bent’s rule we expect high s-character lone pairs of main group atoms. For example, singlet  $CH_2$  has a gross hybridization of  $sp^2$ . However the geometry is consistent with greater s-character ( $sp^{0.580}$ ) in the lone pair relative to the C–H bonds ( $sp^{4.445}$ ). Similarly, the geometry of triplet  $CH_2$  is consistent with  $sp^{8.954}$  hybridization of the singly occupied orbitals and  $sp^{1.503}$  hybridization in the C–H bonds. For transition metals, d-orbitals generally lie at lower energies than those of the s-orbitals (as judged by valence orbital ionization potentials<sup>51</sup>). As a result, transition metal lone pairs and radicals prefer high d-character. For example,  $PtH_2$  has gross hybridization of  $sd^5$ ; use of four pure d-orbitals to accommodate the four lone pairs leaves the Pt–H bonds with sd hybridization. Similarly, triplet  $WH_4$  (vide infra) has a gross hybridization of  $sd^5$  with the two unpaired electrons

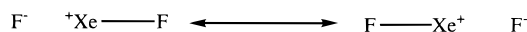
occupying pure d-orbitals and with  $sd^3$  hybridization of the four W–H bonds.

By symmetry, no s-character can be used by  $\pi$ -bonds. Therefore,  $\pi$ -bonds are purely p-character in main group elements and purely d-character in transition metals.

We previously have published a detailed description of the application of these rules to main group elements, including a numeric algorithm for distributing hybridizations.<sup>2</sup>

**Rule 3.** Strong ionic–covalent resonance rationalizes hypervalent bonding; such resonance commonly maximizes at a linear arrangement of the electron pair bond and the ligand localized electron pair.

The simplest hypervalent molecule of the p-block is  $XeF_2$ . Because only four valence orbitals are available at Xe, a minimum first-order VB description must include the two ionic resonance structures shown below. The resonance stabilization of this molecule maximizes at the linear geometry, in accordance with the experimental structure. We put off further discussion of hypervalent molecules to a later section. First we will discuss the geometries of hypovalent and normal valent transition metal hydrides and alkyls in more detail.



#### IV. Hybridization and the Shapes of Normal and Hypovalent Molecules

Devising molecular structures from these rules requires knowledge of the shapes of the bond forming orbitals. We recently have derived hybrid orbital shape functions (Pauling referred to these as “strength functions”)<sup>2</sup> that are generalized for any arbitrary combination of valence s, p, and d atomic orbitals. Figure 1 depicts the shapes of  $sd^n$  hybrids derived from the generalized hybrid orbital function. Table 1 lists the angular preferences associated with common  $sp^n$  and  $sd^n$  hybridizations.

We note that our analysis focuses on *pairwise interactions* of bond forming orbitals.<sup>2</sup> The first hybrid orbital is oriented along the z-axis and an equivalent hybrid is generated in the x–z plane. This method has the disadvantage of not creating a complete set of orthogonal orbitals but carries the significant advantages of (1) creating hybrid orbitals that have unambiguous shapes (using other schemes, the shape of  $sd^n$  hybrids can depend on which d-orbitals are used) and (2) containing expressions suitable for use in molecular mechanics angular terms.<sup>2</sup> Molecular shapes are determined by arranging all ligands to minimize pairwise hybrid orbital overlaps. For example, consider methane and the consequence of  $sp^3$  bond hybridizations. For purposes of orthogonality, each pair of C–H bonds prefers a  $109.5^\circ$  H–C–H bond angle. In accordance with Pauling’s Pair-Defect Approximation,<sup>68</sup> all four H’s are

(41) Hay, P. J.; Wadt, W. R. *J. Chem. Phys.* **1985**, *82*, 299.

(42) Breidung, J.; Thiel, W.; Komornicki, A. *Chem. Phys. Lett.* **1988**, *153*, 76.

(43) Cooper, D. L.; Cunningham, T. P.; Gerratt, J.; Karadakov, P. B.; Raimondi, M. *J. Am. Chem. Soc.* **1994**, *116*, 4414–4426.

(44) Kutzelnigg, W. *Angew. Chem., Int. Ed. Engl.* **1984**, *23*, 272–295.

(45) Martin, J. C. *Chem. Eng. News* **1984**, *62*, 4, 70.

(46) Reed, A. E.; Schleyer, P. v. R. *J. Am. Chem. Soc.* **1990**, *112*, 1434–1445.

(47) Reed, A. E.; Weinhold, F. *J. Am. Chem. Soc.* **1986**, *108*, 3586–3593.

(48) Schleyer, P. v. R. *Chem. Eng. News* **1984**, *62*, 4.

(49) Musher, J. *Angew. Chem., Int. Ed. Engl.* **1969**, *8*, 54–68.

(50) Musher, J. L. *J. Am. Chem. Soc.* **1972**, *94*, 1370–1371.

(51) Landrum, G.; YAEHMOP: Yet Another Extended Hückel Molecular Orbital Package (freely available on the WWW at <http://overlap.chem.cornell.edu:80808/dist/yaehmop.html>); Cornell University: Ithaca, NY, 1997.

(52) Haaland, A.; Hammel, A.; Rypdal, K.; Volden, H. V. *J. Am. Chem. Soc.* **1990**, *112*, 4547–4549.

(53) Pfennig, V.; Seppelt, K. *Science* **1996**, *271*, 626–628.

(54) Morse, P. M.; Girolami, G. S. *J. Am. Chem. Soc.* **1989**, *111*, 4114–4116.

(55) Lappert, M. F.; Raston, C. L.; Skelton, B. W.; White, A. H. *J. Chem. Soc., Chem. Commun.* **1981**, 485–486.

(56) Pulham, C.; Haaland, A.; Hammel, A.; Rypdal, K.; Verne, H. P.; Volden, H. V. *Angew. Chem., Int. Ed. Engl.* **1992**, *31*, 1464–1467.

(57) Piersol, C. J.; Profflet, R. D.; Fanwick, P. E.; Rothwell, I. P. *Polyhedron* **1993**, *12*, 1779–1783.

(58) Stavropoulos, P.; Savage, P. D.; Tooze, R. P.; Wilkinson, G.; Hussain, B.; Motevalli, M.; Hursthouse, M. B. *J. Chem. Soc., Dalton Trans.* **1987**, 557.

(59) Arnold, J.; Wilkinson, G.; Hussain, B.; Hursthouse, M. B. *J. Chem. Soc., Dalton Trans.* **1989**, 2149–2152.

(60) Kolodziej, R. M.; Schrock, R. R.; Davis, W. M. *Inorg. Chem.* **1988**, *27*, 3253–3255.

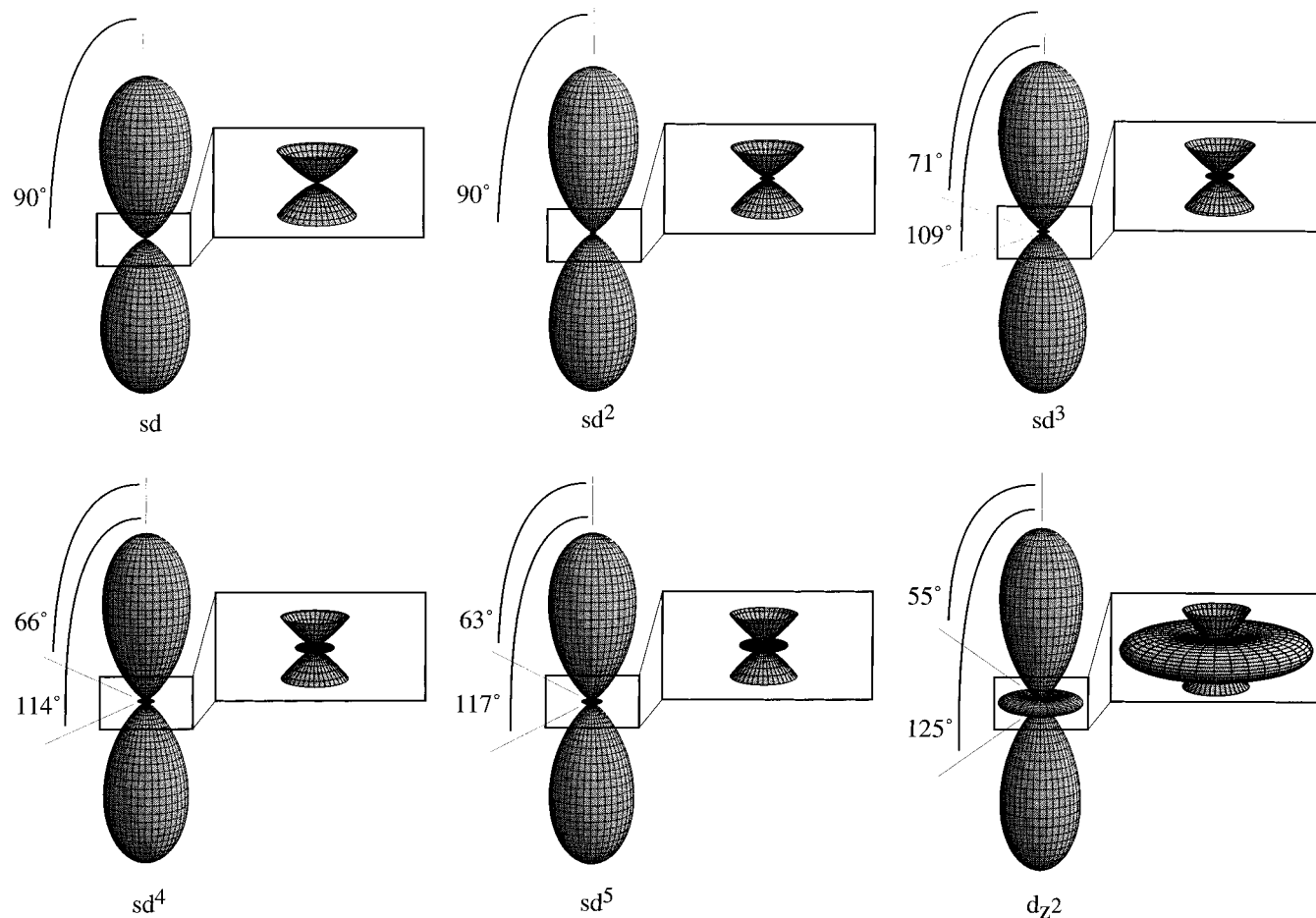


**Figure 1.** Shapes and idealized bond angles for various  $sd$  hybrid orbitals.

arranged about the C atom such that pairwise hybrid orbital orthogonalities are maximized, yielding a tetrahedral geometry.

In predicting the geometries of molecules containing lone pairs or radicals, we consider the hybridizations of the bond-forming orbitals, only. This does not mean that lone pairs are stereochemically inactive; in our model, lone pairs and radicals affect geometry via their influence on the distribution of  $p$  and  $d$  character of the bond forming orbitals. For example, singlet  $\text{CH}_2$  has C–H bond hybridizations of  $sp^{4.445.2}$ . These hybrid orbitals are orthogonal at about  $103^\circ$ , leading to the prediction of a  $103^\circ$  H–C–H bond angle.

**A.  $sd^5$  Bond Hybridization and the Structure of  $\text{WH}_6$ .** Hybridization considerations predict 12-electron  $\text{WH}_6$  to adopt intriguingly complicated molecular shapes. As shown in Table 1, four different molecular geometries accommodate the  $63^\circ$  and  $117^\circ$  H–W–H angular preferences of  $sd^5$  hybridization;<sup>4</sup> two of these have  $C_{3v}$  point group symmetry and two have  $C_{5v}$

(see Table 1). One may view these unusual structures as derived from an icosahedron. Picking any combination of six vertexes such that no two vertexes make a  $180^\circ$  angle generates the two  $C_{3v}$  and two  $C_{5v}$  structures.

Ab initio computations yield structures essentially identical with hybridization predictions. Independent computations performed by Albright and co-workers<sup>26,69</sup> and by Schaefer and co-workers<sup>20</sup> as well as more recent DFT computations by Baker and Tanpipat<sup>27</sup> and ourselves lead to the conclusion that minima of similar energies exist. The two least crowded structures (Table 1, *a* and *c*) are preferred; they differ in energy by about 1 kcal/mol,<sup>26</sup> whereas the more crowded structures are less stable by about 9 kcal/mol for *b*, and 16 kcal/mol for *d*.<sup>26</sup> Qualitative VB theory is incapable of selecting the preferred structure among a set of idealized structures without further considerations. In general, structures that minimize ligand–ligand nonbond interactions will be preferred: for  $\text{WH}_6$  these are structures *a* and *c*.

None of the  $\text{WH}_6$  minima correspond to the octahedral VSEPR prediction. Indeed, ab initio computations suggest a cost of 142 kcal/mol for distortion to the octahedral geometry.<sup>7</sup> Most dramatically, structures *b* and *d* place all of the ligands on one side of a plane normal to the principal symmetry axis that contains the tungsten. From a VB perspective, such geometries are a natural consequence of the  $sd^5$  hybrid orbitals. Similarly we find that small ( $63^\circ$ ) H–M–H bond angles are a natural consequence of hybridization; although it is tempting to suggest that H–H bonding interactions stabilize such small

(61) Cardin, C. J.; Cardin, D. J.; Roy, A. *J. Chem. Soc., Chem. Commun.* **1978**, 899–890.

(62) Arnold, J.; Wilkinson, G.; Hussain, B.; Hursthouse, M. B. *J. Chem. Soc., Chem. Commun.* **1988**, 20, 1349–1350.

(63) Savage, P. D.; Wilkinson, G.; Motevalli, M.; Hursthouse, M. B. *J. Chem. Soc., Dalton Trans.* **1988**, 669–673.

(64) Tooze, R. P.; Stavropoulos, P.; Motevalli, M.; Hursthouse, M. B.; Wilkinson, G. *J. Chem. Soc., Chem. Commun.* **1985**, 1139–1140.

(65) Hay-Motherwell, R. S.; Wilkinson, G.; Hussain-Bates, B.; Hursthouse, M. B. *J. Chem. Soc., Dalton Trans.* **1992**, 3477–3482.

(66) Hitchcock, P. B.; Lappert, M. F.; Smith, R. G.; Bartlett, R. A.; Power, P. P. *J. Chem. Soc., Chem. Commun.* **1988**, 1007–1008.

(67) Hay-Motherwell, R. S.; Hussain-Bates, B.; Hursthouse, M. B.; Wilkinson, G. *J. Chem. Soc., Chem. Commun.* **1990**, 1242–1243.

(68) Pauling, L.; Herman, Z. S.; Kamb, B. *J. Proc. Natl. Acad. Sci. U.S.A.* **1982**, 79, 1361–1365.

(69) Kang, S. K.; Albright, T. A.; Eisenstein, O. *Inorg. Chem.* **1989**, 28, 1611–1613.

bond angles, the H–H distances are much larger ( $>1.7$  Å) than common H–H distances in molecular hydrogen complexes ( $<1.1$  Å).

Further support of the hybridization model has come from experimental<sup>53</sup> and computational<sup>25</sup> analyses of 12-electron  $W(CH_3)_6$  and the crystal structure of the isoelectronic  $[ZrMe_6]^{2-53}$ . These structures are minor distortions of the least congested  $C_{3v}$  geometry, *a*, obtained from hybridization considerations. The preference for this geometry is rationalized readily as the result of minimization of intermethyl steric effects. Also similar to the  $W(CH_3)_6$  is the approximately trigonal prismatic, six-coordinate tris(*o*-xylylene)tungsten molecule.<sup>55</sup> The chelate C–W–C angles for this molecular compound are  $74^\circ$ , similar to the  $73^\circ$  angles of  $W(CH_3)_6$ , but the chelating ligands force the methylene hydrogens to align, increasing steric repulsion to distort the shape to trigonal prismatic.

**B.  $sd^4$  Bond Hybridization and the Structure of  $[WH_5]^+$ .** The  $sd^4$  hybridization of 10-electron  $[WH_5]^+$  leads to idealized H–W–H bond angles of  $66^\circ$  and  $114^\circ$ . From the perspective of our VB model,  $[WH_5]^+$  is electronically frustrated: there is no geometry for which all bond angles formed by the five ligands have the idealized values. Previously we have reported that four local minima (labeled *e*, *f*, *g*, and *h*) have been found by using VALBOND computations; two (*f* and *h*) belong to the  $C_s$  point group and resemble square pyramids.<sup>4</sup> The remaining idealized structures are a pentagonal pyramid *e* ( $C_{5v}$ ) and a distorted pentagonal pyramid *g* ( $C_s$ ). We have since found that *i* and *j*, two  $C_{4v}$  structures, also are minima in VALBOND. With DFT computations we find four local minima, corresponding to structures *g*, *h*, *i*, and *j*, which are listed in Table 2. Neither the DFT structures nor any of the VB-predicted structures resemble the VSEPR predicted trigonal bipyramidal structure.

The occurrence of “electronic frustration” is a clear indicator that the potential energy surface for shape distortions will be complex and soft. The final equilibrium geometry is difficult to predict because it depends on a subtle balance of forces (ligand–ligand Pauli repulsions and electrostatics). Generally, the most symmetrical structure among a set of closely spaced structures is preferred due to optimal balancing of nonbond interactions. For  $[WH_5]^+$ , this leads to the square pyramidal  $C_{4v}$  structure similar to that observed experimentally for  $Ta(CH_3)_5$ .

Although 10-electron  $[WH_5]^+$  and 12-electron  $ReH_5$  have different gross hybridization, we predict similar structures. For  $ReH_5$  the gross hybridization is  $sd^5$ , but the lone pair is purely d in character leaving five Re–H bond orbitals with  $sd^4$  hybridization. DFT computations on  $ReH_5$  yield a  $C_{5v}$  pentagonal pyramid *e* and a  $C_s$  structure *g* similar to two other VALBOND-predicted possible minima. See Table 2 for structural details.

Interestingly, our DFT computations on  $TaH_5$  yield only a single minimum with  $C_{4v}$  symmetry. NBO analysis (vide infra) of the wave function indicates polar Ta–H bonds and a Ta natural charge of +1.2. Correspondingly, the VB picture of  $TaH_5$  has significant contribution from  $[TaH_4]^+ H^-$  resonance structures leading to potential energy surface that is not well described by  $sd^4$  hybridization only. Similarly, gas-phase electron diffraction data of 10-electron  $TaMe_5$  indicate a  $C_{4v}$  structure.<sup>56</sup> The crystal structure of  $Ta(CH_2\text{-}p\text{-}Tol)_5$  exhibits a geometry that is approximately  $C_{4v}$  about the Ta.<sup>57</sup>

**C.  $sd^3$  Bond Hybridization and the Structures of  $[TaH_4]^+$  and  $RuH_4$ .** For  $sd^3$  hybridization, the ideal angles are  $71^\circ$  and  $109^\circ$ . In addition to the tetrahedron two other structures are

consistent with these angles. These structures have  $C_{4v}$  or  $C_{2v}$  point group symmetry. All of these idealized structures can be derived by arranging four ligands at the vertexes of a cube such that no two ligands make a  $180^\circ$  bond angle. Further consideration of interligand steric repulsion favors the tetrahedron as the most stable of the four theoretical minima. By the rules presented above, both 8-electron  $[TaH_4]^+$  and 12-electron  $RuH_4$  have  $sd^3$  bond hybrids. For  $RuH_4$ , two pairs of electrons are accommodated in pure d lone pairs. In addition to the tetrahedral geometry *k* of  $RuH_4$  we find a  $C_{4v}$  square pyramidal minimum *l*, with bond angles of  $69^\circ$  and  $106^\circ$ , which is lower in energy than the tetrahedral local minimum by 8.6 kcal/mol. For  $[TaH_4]^+$  we also find both the tetrahedral *k* and the pyramidal *l* structures. As with the neutral  $TaH_5$ , NBO analysis of  $ZrH_4$  reveals substantial ionic contributions to the electronic structure (vide infra). For  $ZrH_4$  there is a single minimum at the tetrahedral geometry.

All published crystal structures of  $sd^3$  hybridized alkyl and hydrido compounds of which we are aware conform to approximate tetrahedral shapes. These structures range from 8-electron tetraalkyl derivatives of Ti, Zr, and Hf<sup>70</sup> to 12-electron tetraalkyl molecules of Os, Ru, and Ir<sup>+</sup> to 10-electron tetraalkyls of Mo and Cr to 11-electron tetraalkyls of Os<sup>+</sup> and Re (see Table 1).

**D.  $sd^2$  Bond Hybridization and the Structures of  $[ZrH_3]^+$  and  $RhH_3$ .** For both 6-electron  $[ZrH_3]^+$  and 12-electron  $RhH_3$ , qualitative valence bond theory predicts  $sd^2$  bond hybridization and a trigonal pyramidal structure with  $90^\circ$  bond angles. A particularly interesting contrast with VSEPR results occurs in  $[ZrH_3]^+$ : despite the absence of lone pairs, a decidedly nonplanar structure is predicted. VSEPR theory predicts a trigonal planar structure. Our DFT calculations predict a trigonal pyramidal structure with  $103^\circ$  bond angles. For  $RhH_3$ , our DFT results indicate a pyramidal structure with H–Rh–H angles of  $84^\circ$ .

A few crystal structures of nonhypervalent  $sd^2$  hybrids are available: 6-electron  $La(CH(SiMe_3)_2)_3$ <sup>66</sup> is a pyramidal structure with C–La–C angles of about  $109^\circ$  and 12-electron  $Rh(\text{Mesityl})_3$ <sup>67</sup> and  $Ir(\text{Mesityl})_3$ <sup>65</sup> are trigonal pyramids with average C–M–C angles of  $105^\circ$  and  $108^\circ$ , respectively. Such deviations from the idealized angle values of  $90^\circ$  are consistent with the expected interligand repulsions of the bulky ligands.

**E.  $sd$  Bond Hybridization and the Structures of  $[YH_2]^+$  and  $PtH_2$ .** Like  $sd^2$  bond hybridization,  $90^\circ$  angles are predicted for  $sd$  bond hybrids. Thus, both the 4-electron  $[YH_2]^+$  and the 12-electron  $PtH_2$  are predicted to exhibit strongly bent structures. DFT computations of both molecules exhibit bond angles near  $90^\circ$ : for  $PtH_2$  the bond angle is  $85^\circ$ , and for  $[YH_2]^+$  the bond angle is  $103^\circ$ . These results agree with the GVB computations of Low and Goddard for  $PtH_2$  which yielded an  $82.5^\circ$  angle. Similar GVB computations for  $Pt(CH_3)_2$  yielded a  $98^\circ$  C–Pt–C bond angle. To the best of our knowledge, there are no experimental determinations of the structures of normal or hypovalent hydride or alkyl molecules containing  $sd$  bond hybridization.

## V. Consistency of Qualitative VB Theory with Electronic Structure Calculations

One test of simple qualitative models of bonding is consistency with more exact analyses of electron density distributions.

(70) Davies, G. R.; Jarvis, J. A. J.; Kilbourn, B. I. *J. Chem. Soc., Chem. Commun.* 1971, 1511.

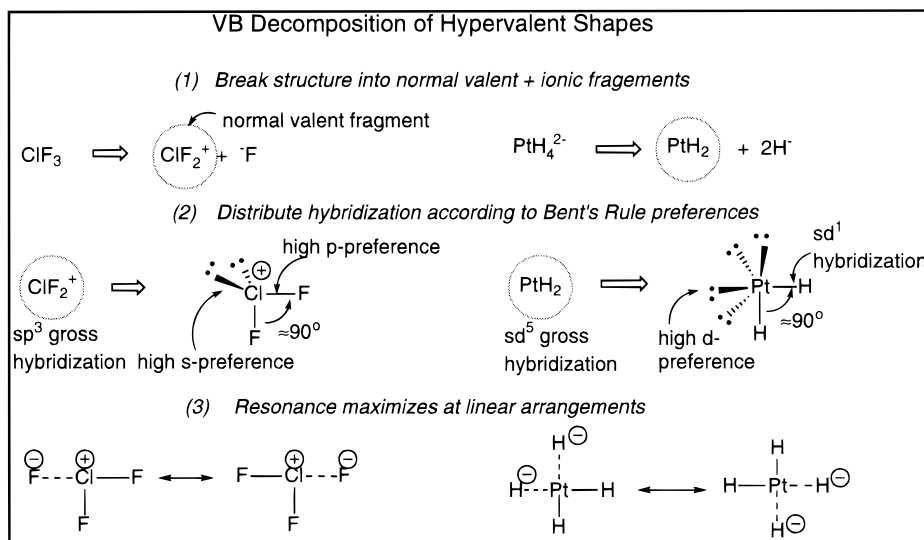


**Figure 2.** A valence bond treatment of  $\text{ClF}_3$  and  $\text{PtH}_4^{2-}$ .

For example, Gillespie and Bader<sup>71</sup> have found strong support for the fundamental concepts of VSEPR theory through analyses of bond critical moments. We have relied primarily on Weinhold and co-workers' Natural Bond Orbital (NBO) analysis<sup>13</sup> as a general method for casting the results of a variety of types of electronic structure calculations into localized bonding terms. As shown in Table 2, simple transition metals are described well by Lewis structures involving electron pair bonds and lone pairs. The average hybridizations of various transition metal hydrides and alkyls determined by NBO exhibit remarkable consistency with the simple rules stated here. For example, each metal forms  $sd^{n-1}$  hybrids where  $n$  is the sum of the bonds + lone pairs + radicals; practically no p-character is used in these hybrids. We also find that transition metal-hydrogen bonds generally are covalent, although more significant departures from pure covalency are observed for the polar covalent bonds of the electropositive early transition metal hydrides (vide infra).

As we have pointed out before,<sup>3</sup> the hybridizations determined by NBO analysis and those used in VALBOND computations are not based on the same criteria. The hybridizations used in this qualitative VB theory represent idealized hybridizations that are applied by using a variant of Pauling's Pair Defect Approximation.<sup>68</sup> In contrast, NBO hybridizations are based on manipulating density matrixes in order to obtain maximum occupancy in a complete set of localized bond orbitals. NBO analysis of  $\text{WH}_6$  in the preferred  $C_{3v}$  geometry yields two sets of W-H hybrids corresponding to the two sets of symmetry equivalent W-H bonds. One set has  $sd^{6.27}p^{0.02}$  hybridization and the other  $sd^{4.08}p^{0.01}$ . (We note that the interpretation of NBO derived p-orbital populations has been questioned by Morokuma.<sup>73</sup>) In contrast, our rules describe  $\text{WH}_6$  as having six  $sd^5$  bond orbitals. Nonetheless, the average NBO hybridization of  $sd^{4.98}p^{0.02}$  closely corresponds to the idealized  $sd^5$  hybridization, thus providing strong support for the simple rules of our qualitative VB method.

It is surprising that valence p-orbitals have so little involvement in metal-hydrogen bonds. We have computed optimized geometries and total energies for  $\text{PtH}_2$ <sup>74</sup> using DFT(B3LYP) methods and the standard Hay and Wadt effective core potential with a Hay and Wadt double- $\zeta$  basis set representation for the 6s, 6p, and 5d orbitals.<sup>39</sup> Additionally, a modified basis set was used, identical to the first one except that the 6p orbitals were omitted. The difference in total energy between the two

computations is only 1.4 kcal/mol. Upon deletion of the 6p valence functions, the bond angle and bond length changes are insignificant; the H-Pt-H angle changes from 85.3° to 85.8° and the Pt-H distance from 1.529 to 1.522 Å. Thus, even for a late transition metal, the valence p functions contribute little to the formation of covalent bonds.

## VI. Qualitative VB Theory and Hypervalent Molecules

Because the qualitative VB model restricts the number of bond-forming orbitals to four and six for p-block and d-block elements, respectively, ionic resonance configurations must be invoked. Each ionic configuration consists of a valence core fragment with all orbitals occupied and the "excess" electron pairs localized on ligands. The molecular geometry is that which maximizes the resonance of these configurations. Historically, the first application of such resonance ideas to transition metal complexes was the rationalization of the trans effect in square planar platinum structures by Yakshin<sup>75</sup> and Syrkin<sup>76</sup> in the 1940s.

Consider two simple examples from the p- and d-blocks. Both 10-electron  $\text{ClF}_3$  and 16-electron  $[\text{PtH}_4]^{2-}$  exceed the available orbital space (Figure 2). The primary resonance configurations have the following forms:  $[\text{ClF}_2]^+ \text{F}^-$  and  $\text{PtH}_2 2\text{H}^-$ . The "core fragments" are  $[\text{ClF}_2]^+$  and  $\text{PtH}_2$ , respectively.  $\text{ClF}_3$  has three ionic configurations, corresponding to placement of the excess electron pair on each of the three ligands, whereas  $[\text{PtH}_4]^{2-}$  has six unique configurations corresponding to  $\text{PtH}_2 2\text{H}^-$ . Because  $\text{ClF}_3$  requires just one ligand-localized electron pair we consider it (as well as  $\text{XeF}_2$ ,  $\text{PF}_5$ , and  $\text{SF}_4$ ) to be "singly hypervalent". By analogy,  $[\text{PtH}_4]^{2-}$ ,  $\text{XeF}_4$ , and  $\text{SF}_6$ , all of which have two excess electron pairs, are "doubly hypervalent". We previously have shown<sup>3</sup> that although it is not easy to see *qualitatively* how the doubly hypervalent formulation of  $\text{SF}_6$

(71) Bader, R. W. *Atoms in Molecules: A Quantum Theory*; Clarendon: Oxford, 1990; Vol. 22.

(72) This work.

(73) Maseras, F.; Morokuma, K. *Chem. Phys. Lett.* **1992**, *195*, 500-504.

(74) Low, J. J.; Goddard, W. A. *J. Am. Chem. Soc.* **1984**, *106*, 6928-6937.

(75) Yakshin, M. M. *C. R. (Dokl.) Acad. Sci. U.R.S.S.* **1941**, *32*, 555-557.

(76) Syrkin, Y. K. *Bull. Acad. Sci. U.R.S.S., Classe Sci. Chim.* **1948**, 69-82.



**Table 3.** Comparison of p- and d-Block Hypervalent Centers

Shape	Dominant Resonance Structures	Examples
Linear		
main group		XeF <sub>2</sub> <sup>28</sup>
transition group		[Au(CH <sub>2</sub> PPh <sub>3</sub> ) <sub>2</sub> ] <sup>+</sup> <sup>82</sup>
T-Shape		
main group		ClF <sub>3</sub> <sup>28</sup>
transition group		[Rh(PPh <sub>3</sub> ) <sub>3</sub> ] <sup>+</sup> <sup>83</sup>
See-Saw		
main group		SF <sub>4</sub> <sup>28</sup>
transition group		[Fe(Naphyl) <sub>4</sub> ] <sup>2-</sup> <sup>84</sup>
Square Plane		
main group		XeF <sub>4</sub> <sup>28</sup>
transition group		[PtH <sub>4</sub> ] <sup>2-</sup> <sup>77</sup>
Mono-vacant Octahedron		
main group		BrF <sub>5</sub> <sup>28</sup>
transition group		[Rh(C <sub>6</sub> F <sub>5</sub> ) <sub>5</sub> ] <sup>2-</sup> <sup>85</sup>
Octahedron		
main group		XeF <sub>6</sub> <sup>28</sup>
transition group		[FeH <sub>6</sub> ] <sup>4-</sup> <sup>86</sup>

leads to an octahedral structure, the *quantitative* VALBOND expression of this formulation yields a rigidly octahedral structure for SF<sub>6</sub>.

The most stable geometry is that which maintains idealized bond angles for the filled valence core fragment while maximizing resonance stabilization among the ionic configurations. In general, maximum resonance occurs when the ligands bearing the excess electron pairs are diametrically opposed in the two configurations. The core fragments, [ClF<sub>2</sub>]<sup>+</sup> and PtH<sub>2</sub>, are bent to approximately 90°. For [ClF<sub>2</sub>]<sup>+</sup> qualitative VB considerations suggest that the sp<sup>3</sup> gross hybridization should be distributed to give high s-character to the lone pairs and high p-character to the Cl–F bond hybrids. As a result of the high p-character of the bonds, [ClF<sub>2</sub>]<sup>+</sup> should be bent to less than 109° in

agreement with the DFT(B3LYP) computed value of 100°. Placing the ligands bearing the excess electron pair opposite one of the core fragment bonds yields the T-shape for ClF<sub>3</sub> and a square planar [PtH<sub>4</sub>]<sup>2-</sup>. These structural predictions are supported by experiment<sup>28,77</sup> and DFT computations for both molecules. As noted by Coulson,<sup>78</sup> resonance among ionic structures with diametrically opposed ligands roughly corresponds to the Pimentel–Rundle three-center four-electron bond.<sup>79,80</sup> More recently, Epiotis has described this arrangement as an “I-bond”.<sup>81</sup>

We previously have published the results of VALBOND molecular mechanics computations on hypervalent molecules of the main group.<sup>3</sup> In this paper we summarize the application of these concepts to hypervalent transition metal hydrides and

alkyls (see Table 3) and highlight the close structural analogies between hypervalent molecules of the p- and d-blocks.

**A. Hypervalent Molecules with sd Bond Hybridization: [PdH<sub>3</sub>]<sup>-</sup>, [PtH<sub>4</sub>]<sup>2-</sup>, and [Mn(CH<sub>3</sub>)<sub>4</sub>]<sup>-</sup>.** As described above, a singly hypervalent molecule with sd bond hybridization such as [PdH<sub>3</sub>]<sup>-</sup> forms a T-shape, similar to that of the main group compound ClF<sub>3</sub>.<sup>3</sup> The sd core fragment prefers a 90° bond angle, and the remaining ligand will be 180° from one of the bonds, maximizing hypervalent resonance (Table 3). We are unaware of any alkyl or hydride crystal structure that is analogous in electron count and number of ligands to [PdH<sub>3</sub>]<sup>-</sup>; the isoelectronic [Rh(PPh<sub>3</sub>)<sub>3</sub>]<sup>+</sup> is an analogue and has a T-shaped geometry.<sup>83</sup>

Doubly hypervalent molecules with sd bond hybridization are common and span both high- and low-spin metal alkyls and hydrides. As expected, these molecules adopt approximately square-planar crystallographic structures; maximum resonance stabilization occurs by placing each of the two ligands bearing excess electron pairs opposite metal–ligand bonds in the core fragments (Table 3). Some examples include the following: 12-electron [MnMe<sub>4</sub>]<sup>-</sup> which has four unpaired electrons and a doubly hypervalent sd hybridized structure;<sup>87</sup> the 15-electron molecules [Ir(C<sub>6</sub>Cl<sub>5</sub>)<sub>4</sub>]<sup>2-</sup>,<sup>85</sup> and [Pt(C<sub>6</sub>Cl<sub>5</sub>)<sub>4</sub>]<sup>-</sup>,<sup>88</sup> with one unpaired electron each; and the 16-electron, diamagnetic [Pt(C<sub>6</sub>Cl<sub>5</sub>)<sub>4</sub>]<sup>2-</sup>,<sup>88</sup> [PtH<sub>4</sub>]<sup>2-</sup>,<sup>77</sup> [AuPh<sub>4</sub>]<sup>-</sup>,<sup>89</sup> [Au(C<sub>6</sub>F<sub>5</sub>)<sub>4</sub>]<sup>-</sup>,<sup>90</sup> [Ag(CF<sub>3</sub>)<sub>4</sub>]<sup>-</sup>,<sup>91</sup> and [Cu(CF<sub>3</sub>)<sub>4</sub>]<sup>-</sup>.<sup>92</sup> Thus, VB theory provides an alternative to crystal field or ligand field theory rationalizations for the common square-planar geometry in 16-electron d<sup>8</sup> complexes. A particularly appealing aspect of the VB analysis of hypervalent molecules is the strong interconnection made between the bonding of square-planar, doubly hypervalent molecules of the d-block and those of the p-block such as XeF<sub>4</sub>.

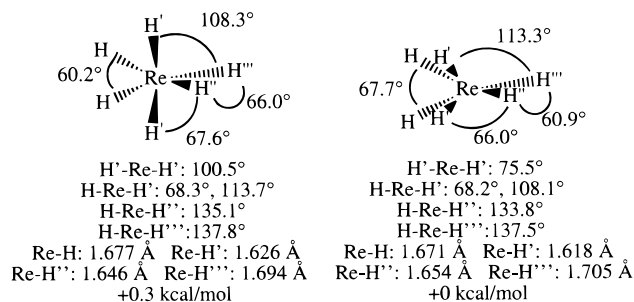
**B. Hypervalent Molecules with sd<sup>2</sup> Bond Hybridization: [RhH<sub>4</sub>]<sup>-</sup>, [Rh(C<sub>6</sub>F<sub>5</sub>)<sub>5</sub>]<sup>2-</sup>, and [FeH<sub>6</sub>]<sup>4-</sup>.** As described in the previous section, an sd<sup>2</sup> bond hybridization leads to trigonal pyramidal structure with angles of roughly 90°. A singly hypervalent molecule with sd<sup>2</sup> bond hybridization will generate a “seesaw” geometry analogous to SF<sub>4</sub>. For example, the crystallographic structure of 14-electron [Fe(Nap)<sub>4</sub>]<sup>2-</sup> and ab initio computations on the model compound 14-electron [RhH<sub>4</sub>]<sup>-</sup> both exhibit this “seesaw” shape, although the wide angle of the iron compound is only 118°, presumably due to steric

repulsions among the very bulky naphthyl ligands.<sup>84</sup> The DFT minimum for [RhH<sub>4</sub>]<sup>-</sup> is a very clear seesaw geometry, with H–Rh–H angles of 178°, 89°, and 85°.

Doubly hypervalent molecules with sd<sup>2</sup> bond hybridization form mono-vacant octahedra (square pyramidal structures with bond angles of approximately 90° and 180°) in analogy with the doubly hypervalent, five-coordinate molecules of the p-block such as 12-electron BrF<sub>5</sub>. A crystallographically characterized example that contains no unpaired electrons is 16-electron [Rh(C<sub>6</sub>F<sub>5</sub>)<sub>5</sub>]<sup>2-</sup>.<sup>93</sup> The 13-electron molecule [CrPh<sub>5</sub>]<sup>2-</sup>,<sup>94</sup> in which the core fragment contains three unpaired electrons and three electron-pair bonds, also exhibits a mono-vacant octahedral structure.

Triply hypervalent molecules based on sd<sup>2</sup> hybridization form the familiar octahedral shape. This structure results from three 3c-4e<sup>-</sup> bonds, all at right angles to each other. XeF<sub>6</sub>, which is slightly distorted from octahedral geometry, is a main group analogue. Crystallographically characterized 18-electron hydride and methyl compounds forming this shape include [FeH<sub>6</sub>]<sup>4-</sup>,<sup>86</sup> [RhMe<sub>6</sub>]<sup>3-</sup>,<sup>95</sup> and [IrMe<sub>6</sub>]<sup>3-</sup>.<sup>95</sup> Open-shell, 15-electron analogues that have been crystallographically characterized include [CrMe<sub>6</sub>]<sup>3-</sup>,<sup>96</sup> and [MnMe<sub>6</sub>]<sup>2-</sup>.<sup>97</sup>

**C. Hypervalent Molecules with sd<sup>4</sup> Bond Hybridization: Re(CH<sub>3</sub>)<sub>6</sub> and ReH<sub>6</sub>.** The simplest hypervalent molecule with an sd<sup>4</sup> bond hybridization is the 13-electron ReH<sub>6</sub> radical, with an 11-electron [ReH<sub>5</sub>]<sup>+</sup> core fragment comprising five sd<sup>4</sup> bond hybrids and one pure d radical. Qualitatively, one anticipates a structure with acute bond angles near 66° and obtuse angles opened from 114° due to maximization of resonance. DFT computations lead to the two minima (there may be others) shown below.



(77) Bronger, W.; Müller, P.; Schmitz, D.; Spittank, H. *Z. Anorg. Allg. Chem.* **1984**, *516*, 35–41.

(78) Coulson, C. A. *J. Chem. Soc.* **1964**, 1442.

(79) Pimentel, G. C. *J. Chem. Phys.* **1951**, *19*, 446–448.

(80) Rundle, R. E. *Rec. Chem. Prog.* **1962**, *23*, 194–221.

(81) Epiotis, N. D. *Deciphering the Chemical Code*; VCH Publishers: Inc.: New York, 1996.

(82) Cerrada, E.; Gimeno, M. C.; Laguna, A.; Laguna, M.; Orera, V.; Jones, P. G. *J. Organomet. Chem.* **1996**, *506*, 203.

(83) Yared, Y. W.; Miles, S. L.; Bau, R.; Reed, C. A. *J. Am. Chem. Soc.* **1977**, *99*, 7076.

(84) Bazhenova, T. A.; Lobkovskaya, R. M.; Shibaeva, R. P.; Shilova, A. K.; Gruselle, M.; Leny, G.; Deschamps, E. *J. Organomet. Chem.* **1983**, *244*, 375–382.

(85) Garcia, M. P.; Jimenez, M. V.; Oro, L. A.; Lahoz, F. J.; Tiripicchio, M. C.; Tiripicchio, A. *Organometallics* **1993**, *12*, 4660–4663.

(86) Bau, R.; Ho, D. M.; Gibbins, S. G. *J. Am. Chem. Soc.* **1981**, *103*, 4960–4962.

(87) Morris, R. J.; Girolami, G. S. *Organometallics* **1991**, *10*, 792.

(88) Usón, R.; Forniés, J.; Tomás, M.; Menjón, B.; Sünkel, K.; Bau, R. *J. Chem. Soc., Chem. Commun.* **1984**, 751–752.

(89) Markwell, A. J. *J. Organomet. Chem.* **1985**, *293*, 257.

(90) Murray, H. H.; Fackler, J. P. J.; Porter, L. C.; Briggs, D. A.; Guerra, M. A.; Lagow, R. J. *Inorg. Chem.* **1987**, *26*, 357.

(91) Geiser, U.; Schlueter, J. A.; Williams, J. M.; Naumann, D.; Roy, T. *Acta Crystallogr. Sect. B: Struct. Sci.* **1995**, *51*, 789.

(92) Geiser, U.; Schlueter, J. A.; Williams, J. M.; Naumann, D.; Roy, T. *Acta Crystallogr. Sect. B: Struct. Sci.* **1995**, *51*, 789.

The primary difference between the two structures is the H'–Re–H' angle, which is obtuse in the left structure and acute in the right one. Although no experimental data for ReH<sub>6</sub> exist, Seppelt has reported the X-ray crystallographic structure of Re(CH<sub>3</sub>)<sub>6</sub>.<sup>53</sup> This structure exhibits a structure that is a slightly distorted trigonal prism with C–Re–C bond angles of ~86° and ~80° between C<sub>3</sub> symmetry related carbons.

**D. Hypervalent Molecules with sd<sup>5</sup> Bond Hybridization: [WH<sub>7</sub>]<sup>-</sup>.** Approximate bonding structures for the sd<sup>5</sup> hybridized hypervalent compound, [WH<sub>7</sub>]<sup>-</sup>, can be constructed from the normal valent WH<sub>6</sub> core. [WH<sub>7</sub>]<sup>-</sup> is a singlet with a 14e<sup>-</sup> formal electron count, and so is singly hypervalent. Addition of H<sup>-</sup> to either of the C<sub>5v</sub> structures (c or d from Table 1) should lead to a strainless seven-coordinate C<sub>5v</sub> structure. In contrast, addition of H<sup>-</sup> along the C<sub>3</sub> axis of the C<sub>3v</sub> structures (a and b from Table 1) leads to C<sub>3v</sub> structures that lack a linear

(93) Garcia, M. P.; Oro, L. A.; Lahoz, F. J. *Angew. Chem., Int. Ed. Engl.* **1988**, *27*, 1700–1701.

(94) Müller, E.; Krause, J.; Schmiedeknecht, K. *J. Organomet. Chem.* **1972**, *44*, 127–140.

(95) Hay-Motherwell, R. S.; Wilkinson, G.; Hussain, B.; Hursthouse, M. B. *J. Chem. Soc., Chem. Commun.* **1989**, 1436–1437.

hypervalent resonance stabilization. Thus we anticipate a small amount of electronic strain in the  $C_{3v}$  structures.

We have found two DFT(B3LYP) geometries that are true minima; these correspond to the two  $C_{3v}$  structures described above. These two minima are close in estimated energy, with the eclipsed lower in energy by about 3 kcal/mol. Interestingly, for  $[\text{WH}_7]^-$  the “strainless”  $C_{5v}$  geometry is 9 kcal/mol higher in energy than the  $C_{3v}$  eclipsed geometry and is not a local minimum. Presumably this is due to adverse steric and electrostatic interactions between the pentagonal array of pseudoequatorial H's and the proximal axial H, as was found for  $\text{WH}_6$  structure *d*.

## VII. Qualitative VB Descriptions of Hypervalency and *ab Initio* Electron Density Distributions

Unlike the normal and hypovalent molecules discussed in sections IV and V, single resonance structures do not describe well the electron density distributions of hypervalent transition metal molecules. Consider the three simple hydrides  $[\text{PdH}_3]^-$  (14-electron),  $[\text{PtH}_4]^{2-}$  (16-electron), and  $[\text{RhH}_4]^-$  (14-electron). According to NBO analyses of DFT(B3LYP) density matrices, a single Lewis structure accounts for only 98.6%, 98.4%, and 98.4%, respectively, of the electron density. For comparison, normal and hypovalent structures, single NBO structures of Table 2, on average account for 99.7% of the electron density in the NBO formalism.

It is interesting to note that hypervalent molecules of the transition metal series do not accommodate the “excess” electron density through the use of valence p-orbitals. As found by Magnusson<sup>16</sup> for the d-orbitals of hypervalent main group complexes, valence p-orbitals in transition metal complexes act primarily as polarization functions. Three observations support the impotence of valence p-orbitals in hypervalent transition metal bonding. (1) The natural atomic configuration of the DFT(B3LYP) density matrix of  $[\text{PtH}_4]^{2-}$ ,  $s^{0.98}d^{9.31}p^{0.27}$ , exhibits much less p-character than required for traditional  $dsp^2$  hybridization. (2) NBO analysis finds that the best single resonance structure contains just two Pt–H bonds, each having  $sd^{1.24}p^{0.13}$  hybridization at the Pt. (3) Optimization of the molecular geometry after complete removal of the valence p-orbitals from the basis set yields only minor changes in Pt–H bond lengths (from 1.694 to 1.689 Å) and a modest increase in total energy (+0.073 hartrees, or about 0.06% of the calculated total energy). In summary, these natural orbital based methods demonstrate that hypervalency in the d-block shares many features with hypervalency of the p-block, including a need for multiple resonance structures, maximization of resonance stabilization at linear geometries for 3c-4e<sup>-</sup> bonding, and the lack of involvement of high lying valence orbitals.

## VIII. Further Applications

**A. Core Polarizations and the Shapes of Metal Hydrides and Alkyls.** Simple metal hydrides and alkyls exhibit unusual structures. One alternative explanation that has been offered by Gillespie and co-workers,<sup>98,99</sup> and by others,<sup>100</sup> is a core polarization model. In this model the interaction of the negative charge of the ligands with the core causes the outer shell of the

**Table 4.** A Comparison of Optimized Geometries for  $\text{WH}_6$  Obtained with a Nonpolarizable Effective Core Potential and with a Polarizable Penultimate Shell (in parentheses)

isomer of $\text{WH}_6$	W–H distance (Å)	H–W–H angle (deg)
<i>a</i> ( $C_{3v}$ )	1.73 (1.65)	63 (64)
	1.79 (1.71)	68 (68)
<i>b</i> ( $C_{3v}$ )		114 (113)
		120 (121)
	1.71 (1.67)	61 (63)
	1.79 (1.72)	69 (70)
<i>c</i> ( $C_{5v}$ )		120 (120)
		121 (124)
	1.75 (1.70)	65 (65)
	1.82 (1.75)	114 (114)
<i>d</i> ( $C_{5v}$ )		120 (121)
		65 (66)
	1.69 (1.66)	66 (68)
	1.75 (1.70)	121 (124)

core to partially localize into pairs. The negatively charged ligands tend to avoid these electron domains, yielding an angular geometry.

We have adapted the methods of Kaupp et al.<sup>100</sup> in using different effective core potentials (ECP's) to probe the effect of core electron flexibility on molecular geometry. These authors have found that  $\text{BaH}_2$  exhibits little driving force to bend when the core electrons are described by a nonpolarizable ECP. Introducing polarizability to the ECP restores the bent geometry.

The  $\text{WH}_6$  molecule was analyzed to look for core polarization effects as follows. Two basis sets were used; in the first, all core electrons were represented by an ECP, leaving only the 6s, 5d, and 6p orbitals free to be nonspherically symmetric. The second used an ECP such that the 5s and 5p (as well as the valence 6s, 5d, and 6p) shells were described explicitly. It is expected that any core polarization effects would result predominantly from the outermost core electrons, so that the second ECP should lead to geometries that differ significantly from those obtained with the first ECP.

Both ECP's (valence only and valence plus penultimate shell) yield similar, nonoctahedral shapes (Table 4) for all four minima of the  $\text{WH}_6$  molecule. As expected, the W–H distances increase upon freezing of the penultimate shell. Significantly, the H–W–H angles of the minimized structures are virtually identical for the two computations. Thus, the molecular shape of  $\text{WH}_6$  appears to be insensitive to the amount of polarizable core electron density.

Other features distinguish  $\text{WH}_6$  from the alkaline earth halides and hydrides. In  $\text{WH}_6$  (and most of the hydrides examined in this paper) the metal–hydrogen bonds exhibit little charge transfer (see Table 3) whereas the alkaline earth halides and hydrides are decidedly ionic in nature. Second, the energy for linearization of alkaline earth hydrides typically is quite low (5–6 kcal/mol).<sup>100</sup> In contrast, the distortion energy for “linearizing” the three pairs of H–W–H bonds to give an octahedron is estimated to cost approximately 142 kcal/mol.<sup>7</sup> Thus, although core polarization effects may be important for metal hydrides with substantially ionic M–H bonds, orbital hybridization better rationalizes the structures and energetics of most transition metal hydrides.

**B. Limitations of the Qualitative VB Scheme.** The rules presented above implicitly assume that the molecule under consideration (1) is predominately covalent and (2) has valence s and p or valence s and d orbitals with similar radial extents. Groups 6–11 of the second and third transition series have Pauling electronegativities<sup>14</sup> (1.93–2.38, second row; 2.2–2.54,

(96) Krausse, J.; Marx, G. *J. Organomet. Chem.* **1974**, *65*, 215–222.

(97) Morris, R. J.; Girolami, G. S. *J. Am. Chem. Soc.* **1988**, *110*, 6245–6252.

(98) Gillespie, R. J.; Robinson, E. A. *Inorg. Chem.* **1995**, *34*, 978.

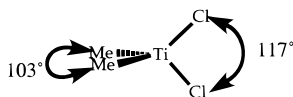
(99) Bytheway, I.; Gillespie, R. J.; Tang, T.-H.; Bader, R. F. W. *Inorg. Chem.* **1995**, *34*, 2407.

(100) Kaupp, M.; Schleyer, P. v. R.; Stoll, H.; Preuss, H. *J. Chem. Phys.* **1991**, *94*, 1360.

third row) that are similar to those of H (2.20) and C (2.55). Thus we expect these transition metals to form nonpolar covalent bonds with hydride and alkyl ligands. In contrast, the early transition metals and all of the first row transition metals have significantly lower electronegativities (1.1–1.90). Thus we expect the hydride and alkyl complexes of these metals to have polar M–H and M–C bonds, hence, significant contributions from ionic resonance structures. Transition metal complexes with highly electronegative ligands or donor–acceptor bonding may not be described well with the simple rules presented here.

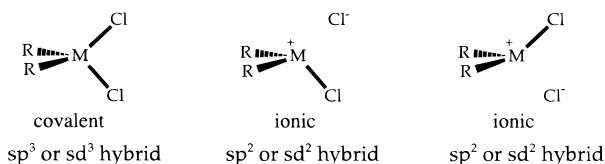
The average radii<sup>101</sup> of the valence s and d orbitals for the second and third row transition metals are much more similar (ratio of 5s/4d and 6s/5d  $\langle r \rangle$ 's range from 1.8 to 2.5 for Y–Ag and 1.8–2.3 for Hf–Au) than those for the first row (4s/3d  $\langle r \rangle$  ratios vary from 2.4 to 3.2 for Sc – Cu). Hybridization is a more effective for the second and third row metals than for the first because of the better match of s and d radial distributions. As a result, hybridization prescriptions work less well for first row transition metals. For example, for CrH<sub>6</sub> Albright and co-workers<sup>26</sup> found 10 minima encompassing structures similar to WH<sub>6</sub> as well as Cr(H<sub>2</sub>)<sub>3</sub> and other mixtures of H<sub>2</sub> and H ligands. We rationalize the differences between Cr and W hexahydrides as the result of weaker Cr–H than W–H bonds due to less effective sd hybridization.

**C. Transition Metal Complexes and Bent's Rule.** Frenking and co-workers<sup>102</sup> recently have suggested a modified version of Bent's rule. In their modification, the rule states that "The energetically lower lying valence orbital concentrates in bonds toward electropositive substituents".<sup>102</sup> They conclude that, for the Ti–C bonds of TiMe<sub>2</sub>Cl<sub>2</sub>, "a higher d character means a smaller bond angle".<sup>102</sup>



Consider the structure of TiCl<sub>2</sub>Me<sub>2</sub><sup>103</sup> that is shown above. If this molecule is considered to be a purely covalent structure, the gross hybridization is sd<sup>3</sup> and the preferred geometry is T<sub>d</sub> (e.g., TiMe<sub>4</sub>). Frenking's modification of Bent's rule suggests that the more electropositive methyl ligands would have higher d character (sd<sup>3+x</sup>).<sup>102</sup> As seen in Figure 1, increasing the d-character in the Ti–C bonds of an initially tetrahedral complex should lead to an increase in the C–Ti–C bond angles instead of a decrease. By the same reasoning, the electronegative chlorine ligands would have less d character and thus smaller ideal bond angles, rather than the observed larger angles.

Consideration of ionic resonance contributions rationalizes the opposite trends in bond angles seen for TiR<sub>2</sub>Cl<sub>2</sub> and SiR<sub>2</sub>Cl<sub>2</sub> (where R = H or alkyl). A reasonable set of contributing resonance structures is shown below; the two [MR<sub>2</sub>Cl]<sup>+</sup> Cl<sup>–</sup> ionic structures will dominate.



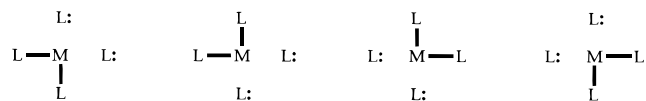
In both the Ti and the Si cases, the s character of the central atom is used in its entirety by each resonance structure, in accordance with Rule 1. The metal–carbon bonds will therefore average more than 25% s character for both the Si and Ti compounds. This increase in s character relative to sp<sup>3</sup>

hybridization widens the Si atom's ideal C–Si–C bond angle from 109°, but for the Ti molecule narrows the ideal C–Ti–C bond angle toward the 90° value preferred by sd<sup>2</sup> hybrids. The metal–chlorine bonds will be a combination of a covalent bond and an ionic resonance form; the widening of the Cl–Ti–Cl bond angle is due to a weakened covalent bending force for this bend, a repulsive ionic interaction between the two Cl atoms, and a narrowing of the C–Ti–Cl bond angle due to the 90° preferred angle in the ionic resonance structure.

In general, we can restate Bent's rule as follows: *Atomic s character will concentrate in covalent bonds (i.e., toward electropositive substituents) for both the main group and the transition group.*

**D. Highly Polar Transition Metal Complexes.** The great majority of well-studied metal complexes have metal–ligand bonds which are substantially more polar than those of hydrides and alkyls. We now briefly discuss some qualitative aspects of the application of VB ideas to metal complexes containing more electronegative ligands.

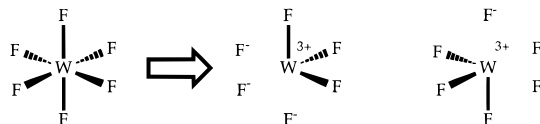
The qualitative VB model of hypervalency invokes ionic structures even when the metal and ligand electronegativities are quite similar. Thus, the inclusion of more electronegative ligands does not require significant changes in the VB description of hypervalent molecules. For example, d<sup>8</sup> square planar complexes are common and encompass a wide variety of ligand types. Whether the complex is [Rh(PMe<sub>3</sub>)<sub>4</sub>]<sup>+</sup>, [PtCl<sub>4</sub>]<sup>2–</sup>, or Pt(NH<sub>3</sub>)<sub>2</sub>Cl<sub>2</sub> we expect that the electronic structure will be dictated by resonances of the form:



(charges and non-resonating lone pairs omitted for generality)

Indeed, Natural Resonance Theory (NRT)<sup>13</sup> analyses support these formulations. Similar considerations apply to [Rh(PPh<sub>3</sub>)<sub>3</sub>]<sup>+</sup>, a 14-electron complex that forms a T-shape<sup>83</sup> (with the largest angle equal to 159°) as expected for a singly hypervalent molecule with sd hybridization.

A covalent picture of WF<sub>6</sub> is inadequate. The bonds are very polar, giving the central tungsten an estimated +2.88 charge from a Mulliken analysis<sup>27</sup> and a Natural Population Analysis<sup>9</sup> suggests +2.57. This suggests that the primary resonance contribution will come from structures with a [WF<sub>3</sub>]<sup>3+</sup> 3F<sup>–</sup> distribution of electrons. These structures have a pyramidal [WF<sub>3</sub>]<sup>3+</sup> core with three sd<sup>2</sup> hybridized bond-forming orbitals:



The hybridization dictates that the facial arrangements of bond pairs will be preferred over other possible [WF<sub>3</sub>]<sup>3+</sup> resonance structures. Resonance among all possible facial arrangements of three bond pairs leads to six equivalent W–F interactions and a strong preference for an octahedral geometry.

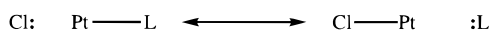
**D. Site Preference and the Trans Influence.** The trans influence is a well-known and much argued phenomenon that

(101) Fischer, C. F. *The Hartree–Fock Method for Atoms*; Wiley: New York, 1977.

(102) Jonas, V.; Boehme, C.; Frenking, G. *Inorg. Chem.* **1996**, *35*, 2097–2099.

(103) McGrady, G. S.; Downs, A. J.; Haaland, A.; Verne, H.-P.; Volden, H.-V. *Inorg. Chem.* **1996**, *35*, 4713.

describes variations in metal–ligand equilibrium properties (such as bond lengths, force constants, coupling constants, etc.) as a function of a trans disposed ligand. Let us consider square planar complexes containing Pt–Cl bonds with a wide variety of trans ligands. Empirically, one finds that the Pt–Cl bond length decreases with the nature of the trans ligand according to the following sequence:  $R_3Si > R_3C = H > CH_2 = R_3P > CO, RNC, C=C, Cl$ . Noting that stabilization of  $3c-4e^-$  bonding interactions requires resonance of the structures shown below, the trans influence is rationalized readily (similar arguments have been put forward by Epiotis<sup>81</sup>). Maximum resonance stabilization requires the energies of the resonating structures to be similar. For less electronegative groups such as silyl, alkyl, and hydride ligands there will be little population of the resonance structure shown below on the right, due to the relatively poor stabilization of an electron pair localized on these groups relative to a Cl ligand. Little resonance stabilization leads to a relatively long (ca. 2.4 Å) Pt–Cl bond. For groups with stabilizations of localized lone pairs that are similar to Cl (i.e. CO, RNC, C=C, Cl) the conditions for maximum resonance stabilization are achieved and the Pt–Cl bonds are relatively short (2.3 Å). Note that this line of reasoning differs from previous arguments<sup>104</sup> in that metal p-orbital involvement and  $\pi$ -bonding effects are de-emphasized in favor of resonance considerations focusing on  $\sigma$ -bonding.



## IX. Conclusions

It recently has become apparent that simple metal molecules commonly exhibit unusual structures when the bonds are primarily covalent. The development of reliable quantum chemical computations has aided the detailed analyses of the geometries and electronic structures of many simple metal-hydride and -alkyl molecules that so far have eluded empirical characterization. Surprisingly, we find that such molecular structures are most simply described by using the concepts of directed valency first proposed by Pauling and Slater at the onset of modern bonding theory. Like the directed valence descriptions of simple main group compounds, Lewis-like structures and rather simple rules for bond hybridization apply to transition metal hydrides and alkyls. Thus, molecules from the d-block that are dominated by covalent bonding are described well by using familiar terms such as hybrid orbitals, lone pairs, resonance, and hypervalence. For such metal molecules,  $sd^n$  hybridization dominates; there is little valence p-orbital participation in bond formation. For nonhypervalent metal alkyls and hydrides, molecular geometries correlate with the shapes of the hybrid orbitals and the minimization of hybrid orbital nonorthogonalities. Although the rules for obtaining appropriate

(104) Huheey, J. E. *Inorganic Chemistry*, 3rd ed.; Harper & Row: Cambridge, 1983.

hybridizations at metal centers arise inductively through analyses of empirical data, it is found that these hybridizations are consistent with localizations of the best available one particle density matrixes from ab initio quantum mechanical computations.

In recent years, considerable evidence has accumulated to indicate that, contrary to Pauling's proposals, hypervalent molecules of the main group do not expand their valency through the use of d-orbitals. Instead, one can view the geometries of hypervalent molecules as arising from resonance stabilization of  $3c-4e^-$  bonding interactions. Metal hydrides and alkyls follow a similar pattern: hypervalent metal centers do not expand valency through the use of valence p-orbitals. Instead, resonance interactions form the most compact description of the electronic and molecular structures. As a result, a remarkable kinship is seen for the structures of main group and transition metal molecules with similar levels of hypervalence. Thus, T-shape, seesaw, square planar, monovacant octahedral, and octahedral geometries are common for both the d- and p-blocks.

At this point it is unclear whether VB theory will provide a useful framework for understanding Werner-type coordination complexes, particularly those of the first transition series. It is likely that the large number of ionic resonance structures and the lower effectiveness of hybridization for first row transition metals will make the approach too clumsy for qualitative applications compared with crystal field or ligand field models. This is an active area of our continuing research into VB descriptions of transition metal complexes.

All of the qualitative bonding considerations presented in this paper can be formulated into algorithms suitable for molecular mechanics computations. Such formulations and their applications to molecular mechanics computations of the structures of hypo-, normal-, and hypervalent molecules will be presented in a subsequent paper.

**Acknowledgment.** This paper is dedicated in fond remembrance of the late Prof. Jeremy Burdett, who inspired us to seek orbital explanations for chemical phenomena. This work was supported in part by grants from the National Science Foundation and the Department of Energy. The authors wish to thank Prof. Frank Weinhold, Prof. Art Ellis, and Prof. Larry Dahl for their critical comments. We also thank Schrödinger, Inc. for a copy of the PS-GVB program. The focus and tenor of this article were greatly improved by the helpful comments of the reviewers.

**Supporting Information Available:** The geometry optimized structures, total energies, vibrational frequencies, natural orbital analyses, and computational methods employed for all ab initio computations (29 pages). See any current masthead page for ordering and Internet access instructions.

JA9710114